ELSEVIER

Materials Science and Engineering A 421 (2006) 217–225

MATERIALS SCIENCE & ENGINEERING A

www.elsevier.com/locate/msea

Creep behavior of carbon fiber/epoxy matrix composites

W.K. Goertzen, M.R. Kessler *

Department of Materials Science and Engineering, Iowa State University, Ames, IA 50011, USA

Received 13 December 2005; accepted 19 January 2006

Abstract

The creep behavior of a carbon fiber/epoxy matrix composite was studied through tensile and flexural creep testing. No creep rupture failures were observed in short-term (less than 1600 h) room temperature tensile creep tests at loads up to 77% ultimate tensile strength (UTS). For elevated temperature flexural creep compliance data taken at isotherms between 30 and 75 °C, the principle of time–temperature superposition held. Master curves were generated by shifting the data by hand and also using the constant activation energy of the glass transition relaxation to estimate the shift factors. It was shown that the constant activation energy assumption worked fairly well, but only for temperatures below the onset T_g of the material. Predictions were made concerning the creep levels at the end of a proposed 50-year design life.

Keywords: Polymer–matrix composites (PMCs); Carbon fibers; Epoxy; Creep; Thermal properties

1. Introduction

In many fiber-reinforced polymer (FRP) composite structures, both the short-term and long-term durability of the material is of importance. While the structure may not fail when subjected to stresses over a short period of time, it may be prone to failure or increased strain when subjected to stresses over an extended period of time. Even if failure does not occur, the slow deformation of the composite material may cause the structure to become less and less effective. The characterization of the long-term performance of FRP composites is especially important because of the viscoelastic behavior of the polymer matrix. FRP matrices exhibit a glass transition, T_g, a temperature above which the properties of the composite degrade significantly. Typically, it is necessary that the application temperature for the composite structure is below the glass transition in order to assure that the mechanical stiffness and creep resistance of the material is satisfactory. However, the glass transition relaxation occurs over a range of temperatures, so creep testing and predictions of long-term creep behavior at particular application temperatures are important so that the material's long-term mechanical performance can be evaluated.

1.1. Theory

Creep is the time-dependent deformation of a material under constant load. While all materials exhibit an initial elastic strain when loaded, this strain may increase over time if the material is susceptible to creep. If a material is perfectly elastic, either linear or non-linear, the strain, ε, will not increase over time and will be a function of the stress, σ, only (for the following set of equations, it is assumed that environmental conditions such as temperature, moisture, etc. are held constant) and is given by

$$\varepsilon = f(\sigma). \tag{1}$$

Elastic solids store energy when they are loaded and use this energy to return to their original shape when unloaded [1]. Liquids, on the other hand, are viscous in that they flow when loaded externally, and the extent to which they deform is time-dependent. However, if a material exhibits behavior that is a combination of viscous and elastic responses to external forces, the material is considered viscoelastic, or time-dependent [1]. The strain of a viscoelastic material will be a function of both stress and time [2] and is expressed by

$$\varepsilon = f(\sigma, t). \tag{2}$$

A viscoelastic material can be characterized as either linear or non-linear with respect to stress. In Eq. (2), $f(\sigma, t)$ can be divided into two functions, one dependent on time, $h(t)$, and one dependent on stress, $g(\sigma)$. This implies that the stress and time

* Corresponding author. Tel.: +1 515 294 3101; fax: +1 515 294 5444.
E-mail address: mkessler@iastate.edu (M.R. Kessler).

0921-5093/$ – see front matter © 2006 Elsevier B.V. All rights reserved.
doi:10.1016/j.msea.2006.01.063

dependencies of the strain are separable [2]. Eq. (2) becomes

$$\varepsilon = g(\sigma)h(t). \tag{3}$$

If it is assumed that the material is linear viscoelastic, the function $g(\sigma)$ would be linear with respect to stress [1]. Likewise, if the material is non-linear viscoelastic, then $g(\sigma)$ would not be linear. For a linear viscoelastic material, the constant associated with $g(\sigma)$ could be included with $h(t)$ in a newly defined function, $S(t)$, which is called creep compliance. Therefore, Eq. (3) becomes

$$\varepsilon = S(t)\sigma. \tag{4}$$

Rearranging Eq. (4), the creep compliance is given by

$$S(t) = \frac{\varepsilon(t)}{\sigma}. \tag{5}$$

If the material is linear viscoelastic, the creep compliance, $S(t)$ will be identical for any given constant stress, $\sigma = \sigma_0$ [2,3]. However, for a material that is assumed to be linear elastic (strain does not increase with time), the creep compliance is simply $\varepsilon/\sigma = 1/E$, where E is the elastic modulus of the material. For a non-linear viscoelastic material, the compliance would be dependent on both time and stress and is given by

$$S(t, \sigma) = \frac{\varepsilon(t, \sigma)}{\sigma}. \tag{6}$$

Creep compliance, $S(t)$, is the desired result from a creep test that measures strain as a function of time for a given stress, regardless of whether the material is linear or non-linear viscoelastic. In contrast to strain data alone, creep compliance is normalized with respect to stress, allowing creep data from tests at differing stress levels to be compared.

Since the desired lifetime of these materials is often measured in tens of years, it is impractical in most cases to conduct long-term creep testing for the entire design lifetime of the material. Thus, much research has been conducted and published on accelerated characterization of creep in composite materials [3,4]. Accelerated models use short-term creep data and corresponding models to predict the long-term behavior of the material in question. Examples of these models include time–temperature superposition (TTSP), the Findley model, the Schapery model, and thermal activation energy theory. Alternatively, it has been shown that dynamic mechanical testing can be used to produce frequency dependent dynamic data that can be transformed into time-domain creep compliance data using an inverse Fourier transform [4].

1.2. Time–temperature superposition

The time–temperature superposition (TTSP) principle is widely used in creep testing of composites to determine the effect of temperature on the creep of FRPs. This theory was originally developed for use with solid polymers [1], but has been expanded for use with fiber-reinforced composites [4]. By the principle of TTSP, the effect of elevated temperature is assumed to be equivalent to stretching the real-time of the creep response by a certain shift factor. Through this assumption, creep compliance is assumed to be a function of time and temperature such that

$$S = S(t, T). \tag{7}$$

Through this method, short-term creep tests at a range of temperatures can be used to generate a transient creep long-term compliance master curve [4]. The length of time of the master curve is in most cases significantly longer than the short-term curves. With this method, the short-term creep curves at each isotherm are plotted on a log scale. A reference temperature is chosen and the other curves are shifted on a log scale by a shift factor, $\log a_T$ [2]. The shift factor is determined graphically by manually lining up the curves or by using a computer program. Alternately, the shift factors can be estimated by determining the activation energy of the glass transition relaxation from the frequency dependence of T_g's measured through dynamic mechanical analysis [5–7].

In the present work, the creep behavior of carbon fiber/epoxy matrix composites used for wrapping and repairing damaged pipelines and pipe work [8–10] is evaluated using both room temperature tensile creep experiments and elevated temperature flexural creep experiments. The generation of creep compliance master curves is explored using both a manual shifting method and using shift factors calculated from the activation energy of the glass transition relaxation. The results are compared, and predictions are made concerning the creep levels that will occur during the design lifetime of the composite material.

2. Experimental

2.1. Materials

The composite specimens were constructed using bi-directional woven carbon fiber reinforcement (supplied by Citadel Technologies™, Tulsa, OK). This reinforcement was plain weave fabric consisting of 12 K tow in the warp direction and 3 K tow in the fill direction. The 12 K indicates that there are approximately 12,000 carbon filaments (fibers) in each bundle (tow), while 3 K indicates approximately 3000 filaments per tow. The fabric is fairly coarse, with 4 tows/in. in the warp direction and 8 tows/in. in the fill direction. The matrix material was a two-part epoxy system, SWR/SWH, developed by Citadel Technologies™ (Tulsa, OK). The particular epoxy used is a diglycidyl ether of bisphenol-A (DGEBA) type epoxy cured with an aliphatic amine hardener. The exact chemical structure and nature of the DGEBA epoxy and aliphatic amine hardener used in the SWR/SWH system is proprietary. When stoichiometricly mixed, the epoxy and curing agent produce a hard, highly crosslinked thermoset with high solvent resistance and relatively high impact strength.

2.2. Specimen manufacturing

The epoxy matrix was formulated by mixing the two-part epoxy/amine system using a resin-to-hardener ratio of 2.65:1.

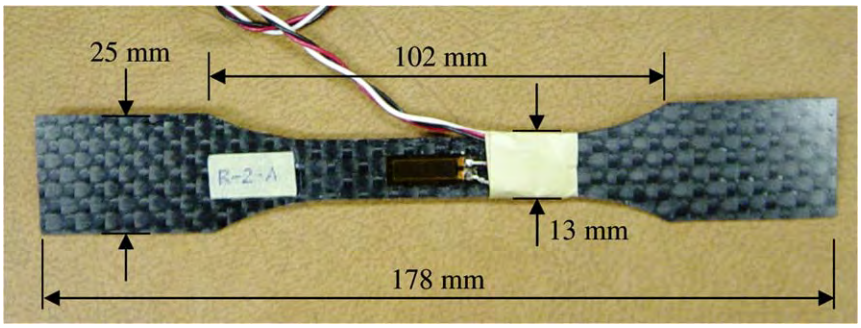

Fig. 1. A gaged specimen used for tensile creep testing (with dimensions in mm).

The plain weave carbon fabric was manually impregnated with the epoxy prepolymer. Composite panels 12 in. × 10 in. were fabricated by hand layup with 2 plies. The layup was done in a Teflon release spray coated pan and a Plexiglas caul plate (sprayed with a Teflon release spray) was placed on top of the panel with less than 3.45 kPa (0.5 psi) of pressure. The Plexiglas was laid down in such a way as to remove the air bubbles from the epoxy and create a uniform surface on the top of the specimen sheet. The panels were cured at room temperature for at least 24 h. The thickness per ply of the composite panels is similar to the thickness per ply of the composite overwrap system used to repair damaged pipelines and pipe work. The fiber volume fraction of the composite was measured to be between 35% and 40%, using both the TGA burnoff and matrix digestion methods in accordance with ASTM D 3171 [11].

Once the panels were cured at room temperature, they were machined to produce dog-bone specimens for tensile creep testing and rectangular specimens for flexural creep testing. The dog-bone test specimen preparation and geometry are acceptable according to ASTM D638 [12]. Vishay MM CEA 06-500UW-120 strain gages were bonded to the gage section of the coupons using M-Bond 200 adhesive. A picture of a typical creep rupture specimen with dimensions is shown in Fig. 1. The thicknesses of the creep rupture specimens ranged from 1.1 to 1.2 mm.

2.3. Equipment

Tensile creep testing was conducted using an in situ creep rupture fixture (see Fig. 2) developed by Lombart and Henshaw at the University of Tulsa [13]. The Dynamic Mechanical Analyzer (DMA) used for the flexural creep testing of the composite

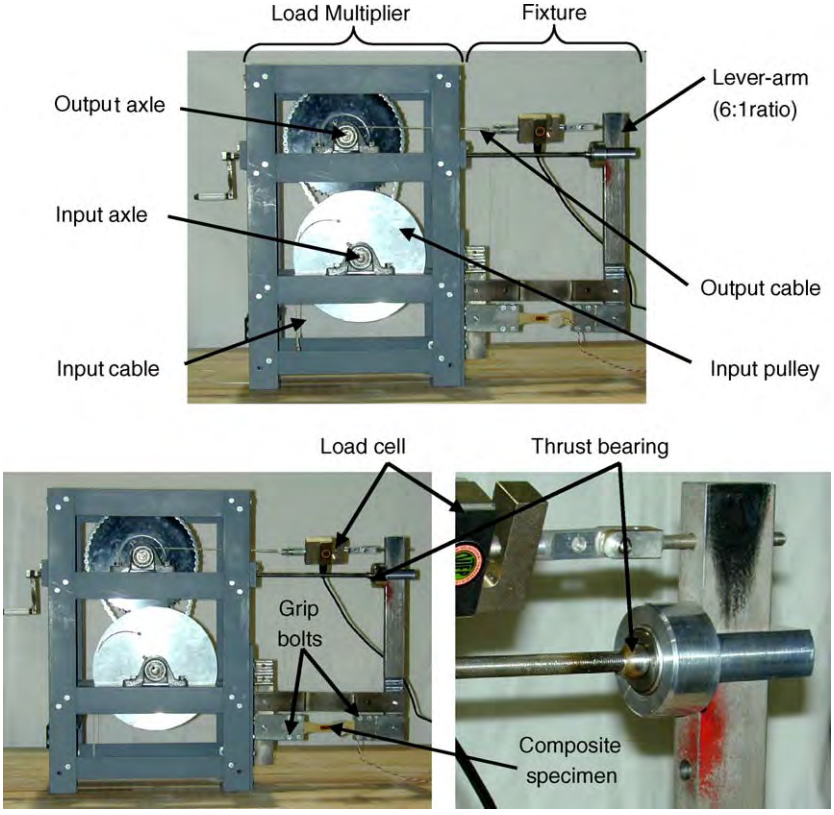

Fig. 2. In situ creep rupture fixture [13].

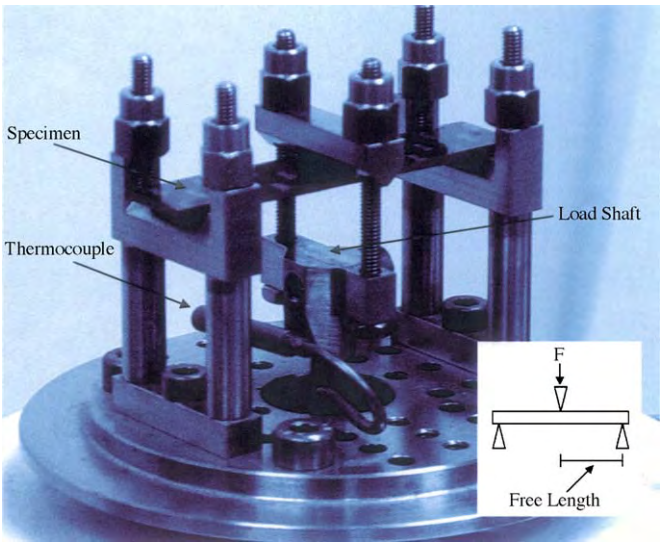

Fig. 3. Three-point bending with constant force.

was a Tritec 2000 DMA manufactured by Triton Technology, Ltd (Keyworth, Notts, UK). It has a load range of −10 to +10 N and a displacement range of −1 to 1 mm. A three-point bending mode with a free length of 20 mm was used. The three-point bending DMA fixture is shown in Fig. 3.

2.4. Experimental procedure—tensile creep

The procedure used for the tensile creep testing was a revised version of the testing procedure developed by Lombart [13]. The fixture uses a load multiplier to achieve a 187:1 ratio of load of the specimen to weight hung from the machine. The first major load multiplication is done through a system of pulleys and the second load multiplication is done by a lever arm with an output to input load ratio of 6:1. The load is monitored by 4400 N load cell attached to the output cable that is attached to the lever arm (see Fig. 2). Strain, load, temperature, and humidity are recorded by a data acquisition system with LabVIEW software.

Before loading the specimen in the grips, the lever-arm is placed in a vertical position and the threaded rod is turned until it contacts the thrust bearing (see Fig. 2). The specimen is then placed in the grips and the bolts are tightened to a specified torque. Then, the strain gage is calibrated using the LabVIEW software. Next, the weights are attached to the cable to achieve the desired output load. After starting the recording of data, the specimen is loaded by slowly turning the threaded rod until it does not touch the lever arm. As the lever arm deflects, however, the weights must be raised to prevent them from hitting the ground. This is done by engaging the clutch and rotating the input pulley.

2.5. Experimental procedure—flexural creep

Creep and creep recovery cycles were conducted at isotherms between 30 and 75 °C in intervals of 5 °C. For each isotherm, a constant force of 4 N (corresponding to a stress of 32 MPa (4.7 ksi)) was applied for 3 h, followed by a 3 h recovery period. The load was applied at a rate of 24 N/min, and data points were taken every 30 s, with a measurement delay time of 30 s. Prior to testing, the specimen was post-cured twice at 60 °C (140 F) for times of 24 and 72 h. The T_g of the material at this cure state is 82 °C for the tan delta peak method and 63 °C for the onset method, measured by DMA at 1 Hz and 2 °C/min.

3. Results and discussion

3.1. Tensile creep testing

In initial testing, four-layer composite specimens were used and slippage in the grips was experienced, causing erroneous results. This was due to the large average loads placed on the specimens, which were around 13,300 N (3000 lbf). To eliminate grip slippage, loads were reduced by using two-layer specimens instead of four-layer specimens, new fine tooth grips were used, and the bolt torque was optimized. As a result of many tests performed with different torques applied, an optimum torque of 10.8 N m (96 lb in.) was found. This torque was applied to each bolt in a star pattern prior to each test.

The ultimate tensile strength (UTS) value for the two-ply composite specimens was determined by tensile testing of specimens from the same batch using a model 810 MTS load frame in displacement control. The average UTS for the 12 K direction was 645 MPa (93.6 ksi) ± 45 MPa (6.5 ksi) (uncertainty is for 95% confidence). All of the creep specimens were tested in the 12 K direction as well. Two successful 1000-plus hour room temperature creep tests were performed at stress levels of 65% UTS (1000 h) and 77% UTS (1600 h) using the new bolt torque. Due to a data acquisition error, data was not recorded for the last 260 h of the 65% UTS test and the last 600 h of the 77% UTS test. However, the specimens stayed loaded for the entire test period without failure before being unloaded and removed from the fixture.

Fig. 4 shows the creep compliance, $S(t) = 1/E(t) = \varepsilon(t)/\sigma(t)$, for the tests conducted at 417 MPa (60.5 ksi) (65% UTS) and 496 MPa (72.0 ksi) (77% UTS). While the compliance values for the 65% UTS test are all larger than that of the 77% UTS test, this

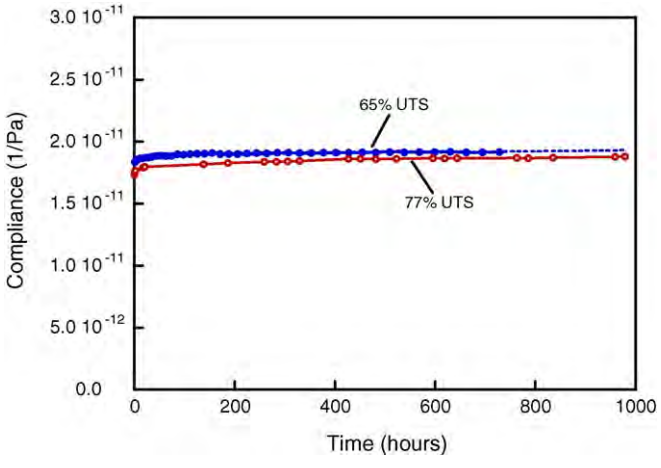

Fig. 4. Tensile creep compliance vs. time, 65 and 77% UTS.

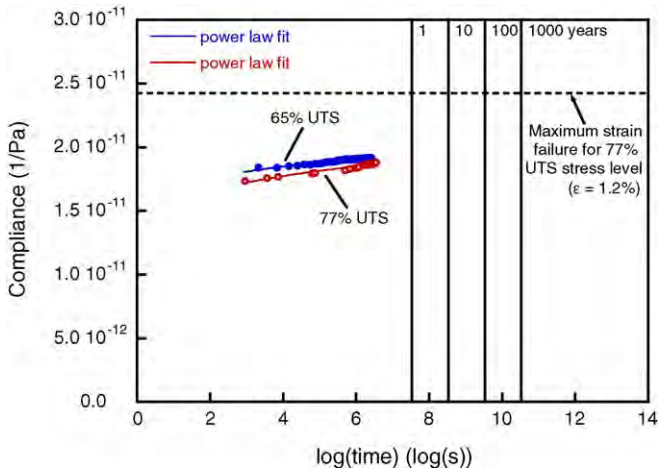

Fig. 5. Tensile creep compliance vs. log time, 65% and 77% UTS.

is due to fluctuations in the modulus of the composite material from specimen to specimen. The uncertainty in the modulus data for this material, as tested by Duell, is approximately 7% [14], but the compliance difference between the 65% and 77% UTS tests at a given time is never larger than 4.6%.

Fig. 5 shows the data for the 77% UTS test and the curve fit for the 65% UTS test on a log time scale. There is little difference between the creep compliance curves for the two stress levels. This would support the notion that the material's behavior was nearly linear viscoelastic in this stress range. It should be noted that the load of 77% UTS nears the limit of the load range for creep rupture testing of this material because of the 14.6% uncertainty in ultimate strength observed during tensile testing by Duell [14]. The curve fits shown are power law relations, used for the characterization of creep of viscoelastic materials under constant stress. According to this model, the compliance is given by $S(t) = kt^n$. The data for both tests follows the power law trend well, with regression coefficients (R^2) of 0.948 and 0.935 for the 65% and 77% UTS tests, respectively. If the creep behavior of the material followed this trend for its entire life, extrapolation of these curve fits would allow predictions to be made concerning the compliance values at the end of a design life, e.g. 50 years. For the 65% UTS test, extrapolation to 438,000 h (50 years) would result in a compliance of 2.00×10^{-11} 1/Pa (1.38×10^{-7} 1/psi), which corresponds to a strain of 0.84%. According to a maximum strain failure criterion, the composite would not reach the ultimate strain of 1.2% during this 50-year period at this 65% UTS. Although the creep failure mechanism for this composite may be quite complex due to the elastic nature of the carbon fibers and the viscoelastic nature of the epoxy matrix, a maximum strain failure criterion is used because of its simplicity and because of a lack of creep rupture data for this particular composite. Using the maximum strain failure criterion in this situation allows for simple comparisons to be made concerning the levels of creep for the material under constant load. For the 77% UTS test, extrapolation of its curve fit to 438,000 h (50 years) would result in a compliance of 1.97×10^{-11} 1/Pa (1.36×10^{-7} 1/psi), which corresponds to a strain of 0.97%. According to a maximum strain failure criterion, the composite would not reach the ultimate strain of 1.2% during this 50-year period at this 77% UTS. However, because of the relatively short test period involved, it would be dangerous to extrapolate these curves and assume that the creep behavior of the composite would continue to behave identically throughout the entire 50-year period. More reliable predictions for such lengths of time can only be made using proven predictive models, such as time–temperature superposition.

3.2. Flexural creep at elevated temperatures

Since it is impractical to conduct creep tests for the entire lifetime of a material, predictions must instead be made concerning the creep levels or time-to-failure at a given load. Since no creep rupture failures were observed in the room temperature tensile creep tests outlined in the previous section, predicting time-to-failure using an extensive creep rupture test program would be impossible without multiple creep fixtures and elevated temperature capabilities. This section will outline the use of time-temperature superposition to predict the lifetime creep behavior of the composite from flexural creep tests at a range of elevated temperatures. The DMA is an ideal apparatus for this type of testing because it is capable of testing at a wide range of temperatures. Although the DMA creep tests will be conducted at low stress levels and in a bending mode, some qualitative creep level predictions can still be made through this method.

Fig. 6 shows the creep compliance versus actual test time for the entire test (the breaks in the data correspond to the recovery periods, in which data was not recorded). Fig. 7 shows the unshifted data on a log time scale, along with the corresponding master curve. According to the principle of time–temperature superposition, each curve was shifted by an appropriate temperature shift factor, $\log a_T$, which is given by

$$\log a_T = \log \frac{t}{t_r} \tag{8}$$

where t is the actual test time and t_r is the reduced time. The reduced time, t_r, is the expanded time scale for the creep master

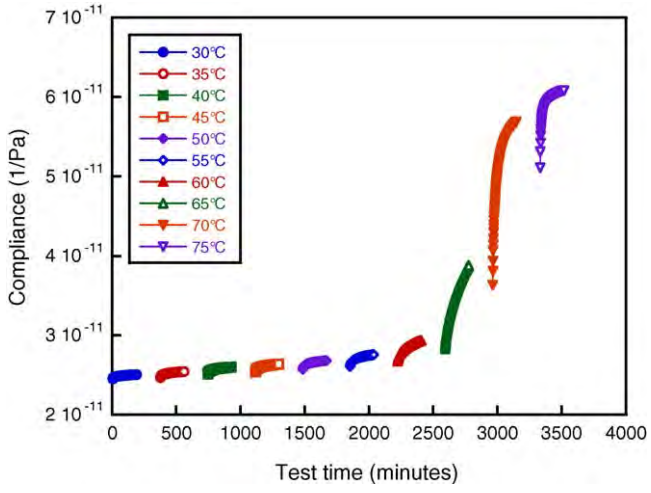

Fig. 6. Compliance vs. actual test time [Data taken every 30 s. Symbols are used to differentiate the curves.].

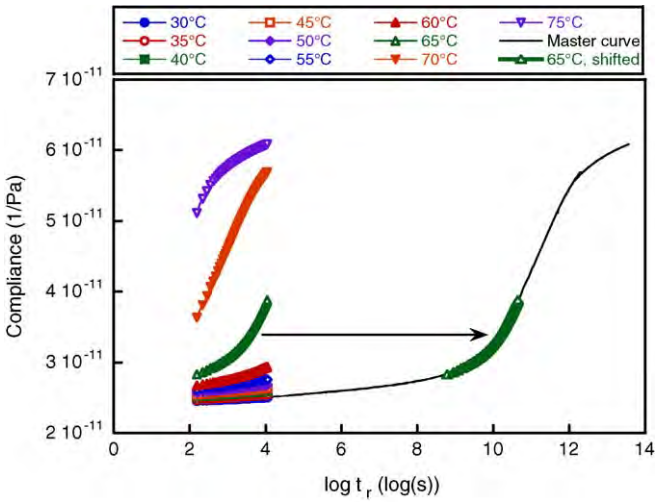

Fig. 7. Unshifted creep compliance data and corresponding master curve for $T_{ref} = 30\,^{\circ}C$, manual shift [Data taken every 30 s. Symbols are used to differentiate the curves.].

curve at an isothermal reference temperature. The reduced time (on a log scale) is given by

$$\log t_r = \log t - \log a_T. \tag{9}$$

The creep compliance curve for the reference temperature, T_{ref}, is left unshifted ($\log a_T$ is zero), while the creep compliance curves for the other temperatures are shifted on the log scale by the shift factor. For temperatures greater than T_{ref}, the curve is shifted to the right ($\log a_T$ is negative), and for temperatures less than T_{ref}, the curve is shifted to the left ($\log a_T$ is positive). The shift factors are chosen by hand so that the isothermal curves overlap.

Alternatively, shift factors can be estimated from the activation energy of the glass transition relaxation. The activation energy of the glass transition relaxation represents the energy barrier that must be overcome for the occurrence of molecular motions causing the transition [15], and was estimated from the frequency dependence of T_g's measured through dynamic mechanical analysis. Fig. 8(a) shown tan delta curves for a range of test frequencies at a heating rate of 2 °C/min. The activation energy is calculated from the slope of a plot of ln(f) versus $1/T_g$, which is shown in Fig. 8(b), by [16]:

$$\Delta H = -R\frac{\mathrm{d}(\ln(f))}{\mathrm{d}(1/T_g)} = -(8.314 \times 10^{-3})(-39.76 \times 10^{3}) = 330.6\,\mathrm{kJ/mol}.$$

Table 1 shows the calculated activation energies for T_g's taken from tan delta and loss modulus peaks for different heating rates (the test specifics and influence of heating rate and T_g measurement method are discussed in our previous work [17]).

The estimation of the activation energy of the glass transition relaxation is quite useful because it can be used to estimate the temperature shift factors for time–temperature superposition without the construction of complete master curves [5–7]. Furthermore, using this estimation, the modulus or compliance of a polymer at the end of its service life (i.e. 50 years) can

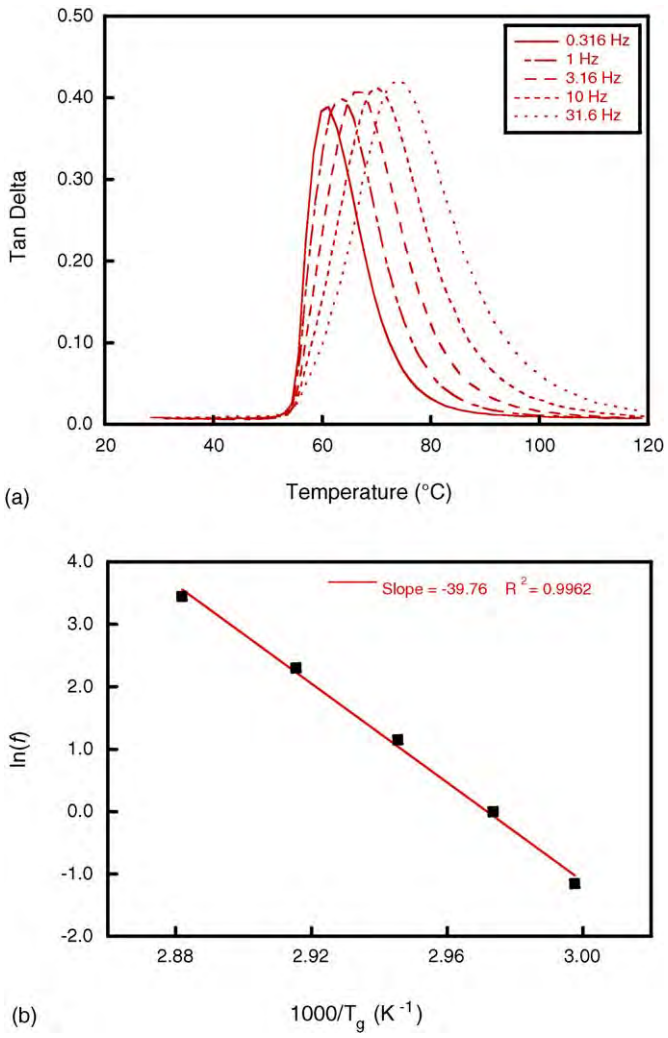

Fig. 8. Calculation of the activation energy of glass transition from the frequency dependence of tan delta curve peak T_g's: (a) tan delta curves for different frequencies at 2 °C/min and (b) variation of T_g as measured by the tan delta peak with the DMA test frequency (2 °C/min). Test frequency, f, in Hz ($\omega = 2\pi f$). The slope of the curve is directly proportional to the activation energy of the glass transition.

be predicted by a single test at an elevated temperature rather than plotting a complete set of master curves [5,7]. In addition, Karbhari and Wang [18] suggest that monitoring the activation energy of the glass transition can be a valuable technique for assessing changes due to environmental exposure and/or aging of the material. Using a constant activation energy assumption, the shift factors are given by [6,7,19]:

$$\log a_T = \frac{\Delta H}{R}\left(\frac{1}{T} - \frac{1}{T_{ref}}\right)\log e, \tag{10}$$

which is derived from the Arrhenius relationship. Eq. (10) holds for temperatures below the T_g of the polymer, where the Williams-Landel-Ferry (WLF) equation is not applicable [6,7]. For this example, the activation energy used to estimate shift factors was the average obtained through the tan delta method, $\Delta H = 324$ kJ/mol (see Table 1). For a reference temperature of 30 °C, the creep compliance master curve generated using shift

Table 1
Activation energies with R^2 values

Heating rate (°C/min)	Activation energies			
	$\Delta H_{\tan\delta}$ (kJ/mol)	R^2	$\Delta H_{E''}$ (kJ/mol)	R^2
0.5	287	0.996	311	0.996
1	312	0.997	342	0.997
2	331	0.996	384	0.987
3	366	0.985	454	0.944
Avg.	324	0.994	373	0.981
S.D.	33.3	5.8E−03	61.9	2.5E−02

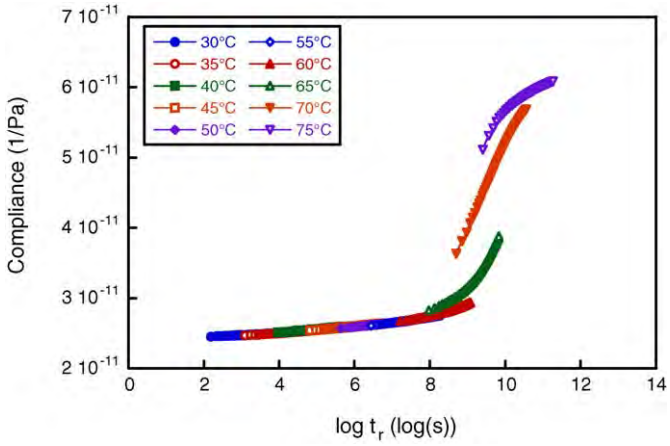

Fig. 9. Creep compliance master curves for $T_{ref} = 30\,^{\circ}C$, constant activation energy [Data taken every 30 s. Symbols are used to differentiate the curves.].

factors estimated from a constant activation energy assumption is shown in Fig. 9.

Fig. 10 shows the shift factors versus the reciprocal of absolute temperature, along with the shift factors obtained using an assumption of constant activation energy. The assumption of constant activation energy gives a linear relationship for $\log a_T$ versus $1/T$ [1]. The manual shift factors follow the linear activation energy shift factor curve well until $1000/T = 3.0$ or $T = 60\,^{\circ}C$, after which the magnitude of the shift factors for the manually shifted data is larger. The fact that the constant activation energy assumption is only valid below T_g, is illustrated in Fig. 9 by the fact that the data for the constant activation energy master curve line up well only through the 60 °C curve. To further illustrate the difference between the shifted data using the manual shift and constant activation energy, Fig. 11 shows an exploded view of the shifted curves for the 30–60 °C isotherms using each method. This data further illustrates the point that the prediction of shift factors using the constant activation energy assumption is only valid for temperatures below the T_g of the material. For this particular case, the cutoff corresponds to the onset T_g, which is

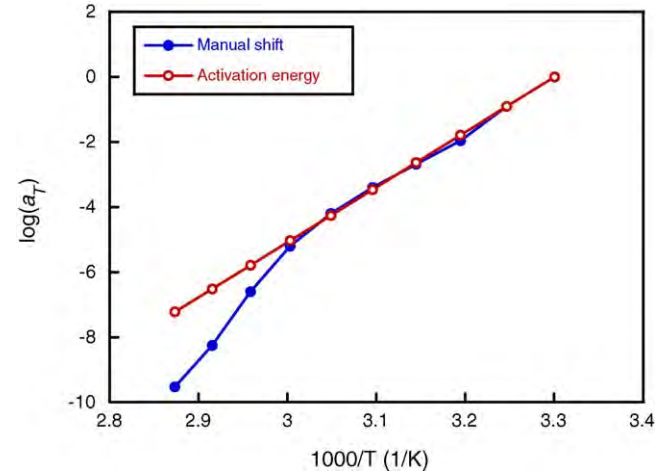

Fig. 10. Shift factors vs. $1/T$ for manual shift and constant activation energy estimation.

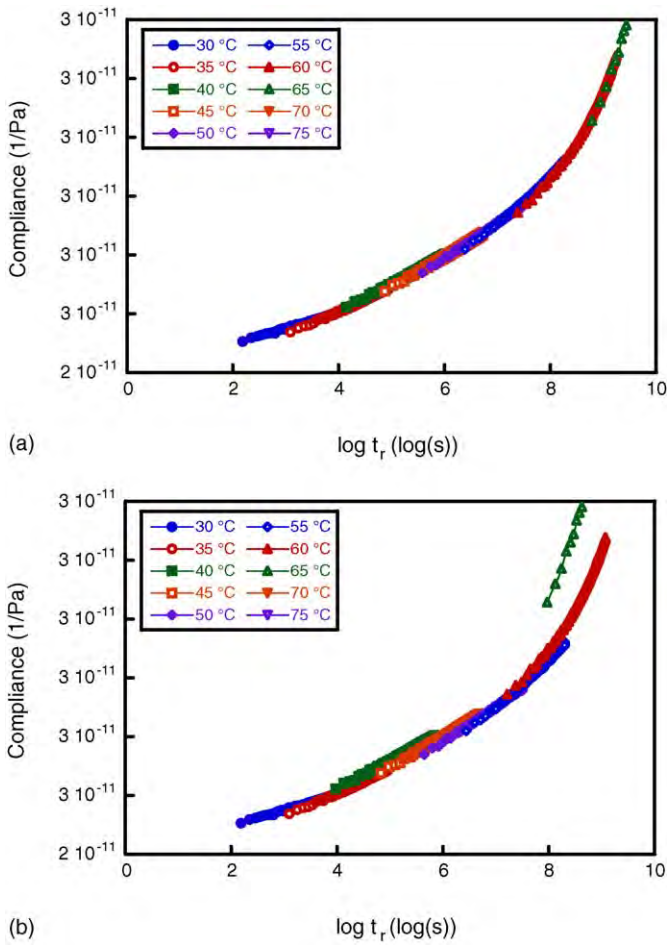

Fig. 11. Master curve exploded view, $T_{ref} = 30\,^{\circ}C$: (a) manual shift and (b) constant activation energy [Data taken every 30 s. Symbols are used to differentiate the curves.].

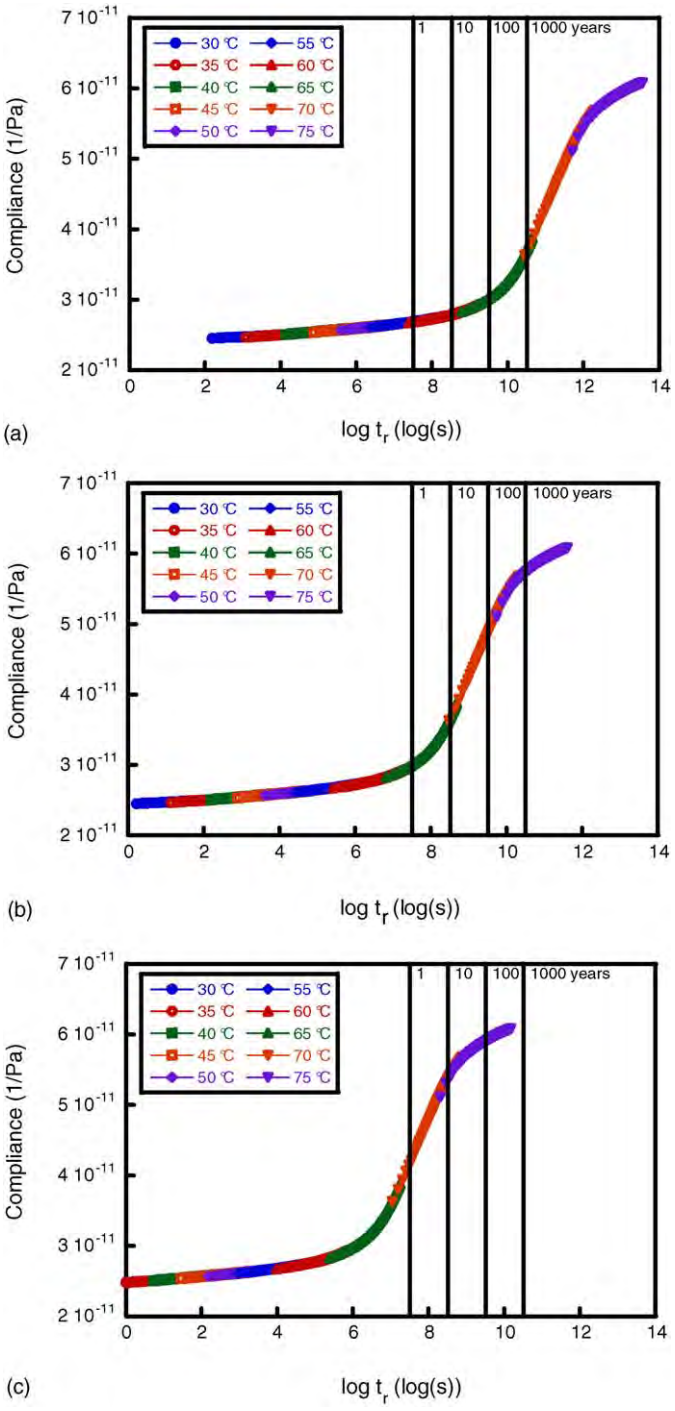

Fig. 12. Master curves with time references in years for: (a) T_{ref} = 30 °C; (b) T_{ref} = 40 °C; (c) T_{ref} = 50 °C [Data taken every 30 s. Symbols are used to differentiate the curves.].

approximately 63 °C (measured by dynamic mechanical analysis).

In order to show the lifetime creep behavior of the material, Fig. 12 shows master curves for reference temperatures of 30–50 °C with lines showing times of 1, 10, 100, and 1000 years. Using the master curves at reference temperatures, T_{ref}, of 30–50 °C, initial predictions of compliance levels for a composite structure operating under constant load at the reference temperature of interest are possible. For these predictions, several assumptions must be made. First, the composite material is assumed to be linear viscoelastic, such that creep compliance levels are the same at any stress level. Second, a maximum strain failure criterion is used to determine failure, and a constant load is assumed. While loads for the application may vary with time, this example is used to make comparisons of creep levels for the simplest case. Finally, since the flexural compliance (and modulus) of the material tested in bending is different from the material's compliance (and modulus) in tension, the ratio of the flexural compliance (and modulus) to the tensile compliance (and modulus) is assumed constant.

Table 2
50-Year design life creep predictions

T_{ref} (°C)	50-Year compliance prediction, S(50 years)[a]		50-Year failure stress (% UTS)	50-Year reduction in modulus (%)
	Flexural (1/Pa)	Tensile (1/Pa)		
30	2.92E−11	2.22E−11	83.9	16.1
40	4.48E−11	3.39E−11	54.8	45.2
50	5.79E−11	4.39E−11	42.4	57.6

[a] Original flexural compliance, S_o: 2.45 E−11 1/Pa; original tensile compliance, S_o: 1.86 E−11 1/Pa.

From each of the master curves at the three different reference temperatures, the flexural creep compliance value was found at a time of 50 years (S(50 years)), a typical maximum design life for a composites pipeline repair system for which the carbon/epoxy composite is intended. By comparing these compliance values to the original compliance values, S_o, the stress level to cause failure at 50 years was calculated. The results are tabulated in Table 2, showing the % UTS level to cause failure at 50 years for each reference temperature. Thus, the stress level required to cause failure at the 50-year point for a constant temperature of 30 °C (86 F) would be approximately 84% UTS. This data point supports the initial prediction made from the results of the tensile creep testing described earlier, which stated that at a 77% UTS stress level, the composite material would not fail in 50 years. However, the original creep compliance level prediction of 1.97×10^{-11} 1/Pa (1.36×10^{-7} 1/psi) for room temperature in the previous section was slightly lower than the 30 °C creep compliance prediction from the time-temperature superposition data, which is 2.22×10^{-11} 1/Pa (1.53×10^{-7} 1/psi). Percent reductions in modulus levels at 50 years are also tabulated in Table 2, such that at 30 °C, the modulus of the material would reduce by approximately 16%, according to the predictions. At 50 °C, the modulus would reduce by 58% over the 50-year period.

While the initial predictions explained above are useful, a safety factor should be built in to all design calculations in order to account for measurement uncertainties and the complexity of the relationship between the material's cure state, T_g, and creep behavior. It would be very useful to conduct further creep testing to validate these predictions. For instance, the most practical check of these predictions would be to test the material at an elevated temperature, such as 50 or 60 °C, for a relatively short test period (i.e. 1000 h) and compare the compliance levels to the master curve for that particular reference temperature. Test

temperatures of this magnitude would be required because the creep levels at room temperature would not be significant enough to make comparisons for any reasonable test period.

4. Conclusions

Creep testing is an important part of the characterization of composite materials. It is crucial to determine long-term deflection levels and time-to-failure for these advanced materials. The tensile creep testing of the composite specimens showed that the carbon fiber composites are resistant to creep rupture under ambient conditions. The creep curves for the two tests were very similar, and no failures were observed at loads of up to 77% of the ultimate tensile strength at times of up to 1600 h. Additionally, the level of creep in the tests was small, such that extrapolation of the creep data would indicate that the material would not fail at the 65% UTS load or the 77% UTS load during a reasonable lifetime.

Further creep testing was performed using a DMA at a range of elevated temperatures in order to make more reliable predictions of long-term behavior using the proven principle of time–temperature superposition. Although tests must be made in bending mode at low stress levels, the DMA provides an efficient method for obtaining creep data at a wide range of temperatures. The principle of time–temperature superposition held for the material tested at isotherms between 30 and 75 °C. Master curves were generated by shifting the data by hand and also using a constant activation energy to estimate the shift factors. It was shown that the constant activation energy assumption held fairly well, but only for temperatures below the onset T_g of the material. A total of three master curves were generated at temperatures of 30–50 °C, and using the compliance data, predictions were made concerning the creep levels at the end of a proposed 50-year design life. The stress levels to induce failure at 50 years ranged from 84% at 30 °C to 42% at 50 °C. The corresponding reductions in modulus over the 50-year period ranged from an 18% reduction over 50 years at 30 °C to a 58% reduction for 50 years at 50 °C.

Acknowledgements

The authors would like to acknowledge and thank Scott Heaton for his help in manufacturing specimens. The technical advice and helpful discussions with Jeffrey Wilson, Joshua Duell, and Roger Walker of Citadel Technologies are also gratefully acknowledged. The authors would also like to thank John Henshaw of the University of Tulsa for the use of his creep rupture fixture and technical advice. This material is based upon work supported under a National Science Foundation Graduate Research Fellowship. Additional funding has been provided by a grant from the Oklahoma Center for the Advancement of Science and Technology (OARS AR03(1)-050).

References

[1] I.M. Ward, D.W. Hadley, An Introduction to the Mechanical Properties of Solid Polymers, John Wiley & Sons, 1993.
[2] J. Nairn, Polymer Characterization, MSE 5473 Class Notes, University of Utah, 2005.
[3] B. Abdel-Magid, R. Lopez-Anido, G. Smith, S. Trofka, Compos. Struct. 62 (2003) 247–253.
[4] D.W. Scott, J.S. Lai, A.-H. Zureick, J. Reinf. Plast. Comp. 14 (1995) 588–617.
[5] A. Kumar, R. Gupta, Fundamentals of Polymer Engineering, 2nd ed., Marcel Dekker, New York, 2003.
[6] R. Li, Mat. Sci. Eng. A-Struct. 278 (2000) 36–45.
[7] A. Rudin, Polymer Science and Engineering, 2nd ed., Academic Press, New York, 1999.
[8] M. Kessler, R. Walker, D. Kadakia, J. Wilson, J. Duell, W. Goertzen, Proceedings of the Biennial International Pipeline Conference (IPC), vol. 2, 2004, pp. 1427–1432.
[9] J. Wilson, M. Kessler, J. Duell, Proceedings of the 2004 ASME Pressure Vessels and Piping Conference PVP, vol. 483, 2004.
[10] J. Wilson, M. Kessler, R. Walker, J. Duell, D. Kadakia, N. Sousa, Proceedings of the 2005 Rio Pipeline Conference and Exposition, October, Rio de Janeiro, Brazil, 2005 (Paper IBP1089_05).
[11] ASTM Standard D 3171-99, Standard Test Methods for Constituent Content of Composite, Materials, American Society for Testing and Materials, West Conshohocken, PA, USA, 2004.
[12] ASTM D638, Standard Test Method for Tensile Properties of Plastics, 2001.
[13] V. Lombart, M.S. Thesis, The University of Tulsa Graduate School, 2002.
[14] J. Duell, M.S. Thesis, The University of Tulsa Graduate School, 2004.
[15] G. LaPlante, P. Lee-Sullivan, J. Appl. Polym. Sci. 95 (2005) 1285–1294.
[16] G. Li, P. Lee-Sullivan, R. Thring, J. Therm. Anal. Calorim. 60 (2000) 377–390.
[17] W. Goertzen, M. Kessler, Compos. Part B-Eng., submitted for publication.
[18] V. Karbhari, Q. Wang, Compos. Part B-Eng. 35 (2004) 299–304.
[19] M. Tajvidi, R. Falk, J. Hemanson, J. Appl. Polym. Sci. 97 (2005) 1995–2004.